Published OnlineFirst March 16, 2016; DOI: 10.1158/1535-7163.MCT-15-0843

Small Molecule Therapeutics

Molecular Cancer Therapeutics

An Unbiased Oncology Compound Screen to Identify Novel Combination Strategies

Jennifer O'Neil[1], Yair Benita[1], Igor Feldman[1], Melissa Chenard[1], Brian Roberts[1], Yaping Liu[2], Jing Li[2], Astrid Kral[1], Serguei Lejnine[1], Andrey Loboda[1], William Arthur[1], Razvan Cristescu[1], Brian B. Haines[1], Christopher Winter[1], Theresa Zhang[1], Andrew Bloecher[1], and Stuart D. Shumway[1]

Abstract

Combination drug therapy is a widely used paradigm for managing numerous human malignancies. In cancer treatment, additive and/or synergistic drug combinations can convert weakly efficacious monotherapies into regimens that produce robust antitumor activity. This can be explained in part through pathway interdependencies that are critical for cancer cell proliferation and survival. However, identification of the various interdependencies is difficult due to the complex molecular circuitry that underlies tumor development and progression. Here, we present a high-throughput platform that allows for an unbiased identification of synergistic and efficacious drug combinations. In a screen of 22,737 experiments of 583 doublet combinations in 39 diverse cancer cell lines using a 4 by 4 dosing regimen, both well-known and novel synergistic and efficacious combinations were identified. Here, we present an example of one such novel combination, a Wee1 inhibitor (AZD1775) and an mTOR inhibitor (ridaforolimus), and demonstrate that the combination potently and synergistically inhibits cancer cell growth *in vitro* and *in vivo*. This approach has identified novel combinations that would be difficult to reliably predict based purely on our current understanding of cancer cell biology. *Mol Cancer Ther; 15(6); 1155–62. ©2016 AACR.*

Introduction

With few exceptions, anticancer monotherapies, whether broadly active cytotoxics or molecularly targeted drugs, have been limited in their ability to elicit robust and durable clinical responses. This is likely attributed to numerous factors including multiple dependencies evolved during tumorigenesis, feedback loops, redundant signaling pathways, and resistance mechanisms, to name a few (1, 2). Combining anticancer therapies has been in practice clinically for over 50 years as one approach to improving upon the responses achieved by single therapies alone (3). Historically, this has been largely an empirical exercise based on preexisting knowledge of oncogenic pathway biologic relationships, or a clinically driven decision based on the preexisting standard of care for a particular cancer. One of the most recent promising combinations showing improved efficacy in the clinic is the combination of trametinib and dabrafenib for the treatment of BRAF-mutant melanoma. The mechanism of the improved efficacy is suggested to involve prevention of negative feedback and resistance (4).

Several large drug sensitivity screening campaigns have been reported. These include the publication of the Cancer Cell line Encyclopedia (CCLE) in which 24 anticancer drugs were screened across 479 cancer cell lines (5) and a study from The Wellcome Trust Sanger Institute in which 130 drugs were screened in 639 cell lines (6). In these studies, known biomarkers of response were validated and biomarker hypotheses were generated demonstrating the power of this approach to aid in drug development. More recently, combination screens have been undertaken to identify novel drug combinations for specific cancer indications, such as melanoma and leukemia, in which resistance to targeted agents has frequently been observed (7–9).

We performed an unbiased screen of 38 compounds in pairwise combinations in a panel of 39 cancer cell lines representing multiple cancer types to identify novel synergistic and efficacious combinations. The results of the screen identified synergy in well-known combinations as well as in novel combinations including the pairing of an mTOR inhibitor (ridaforolimus) and an inhibitor of the DNA damage checkpoint kinase Wee1 (AZD1775). This study demonstrates that unbiased high-throughput screens can be an effective way to discover active, novel synergistic drug combinations.

[1]Merck Research Laboratories, Boston, Massachusetts. [2]Merck Research Laboratories, North Wales, Pennsylvania.

Note: Supplementary data for this article are available at Molecular Cancer Therapeutics Online (http://mct.aacrjournals.org/).

Current address for Y. Benita: Compugen Ltd., Israel; current address for I. Feldman: Epizyme, Cambridge, Massachusetts; current address for B. Roberts: HudsonAlpha Institute for Biotechnology, Huntsville, Alabama; current address for A. Kral: Blueprint Medicines, Cambridge, Massachusetts; current address for W. Arthur: Seattle Genetics, Bothell, Washington; current address for C. Winter: Sanofi, Cambridge, Massachusetts; current address for T. Zhang: Personal Genome Diagnostics, Baltimore, Maryland; and current address for A. Bloecher: Astrazeneca PLC, Waltham, Massachusetts.

J. O'Neil, Y. Benita, and I. Feldman contributed equally to this article.

Corresponding Author: Jennifer O'Neil, Merck Research Laboratories, BMB9-120, 33 Avenue Louis Pasteur, Boston, MA 02115. Phone: 617-992-2542; Fax: 617-992-2412; E-mail: jennifer_oneil@merck.com

doi: 10.1158/1535-7163.MCT-15-0843

Published OnlineFirst March 16, 2016; DOI: 10.1158/1535-7163.MCT-15-0843

Materials and Methods

Drug combination screen

All cell lines were obtained from ATCC or Sigma-Aldrich and used within 6 months of receipt. All cell lines were authenticated at ATCC or Sigma-Aldrich by short tandem repeat (STR) profiling. The high-throughput screen was carried out on the fully automated GNF PolyTarget robotic platform (GNF Systems). Cells were plated in 1,536-well tissue culture-treated plates (Brooks Automation) at 400 cells/well in 10 μL growth media, followed by the addition of 50 nL of compounds in DMSO and incubation at 37°C in 5% CO_2, 95% humidity for 96 hours. The total cell viability of each well was then measured using CellTiter-Glo cell viability reagent (Promega) according to the manufacturer's protocol. The luminescent signal was measured on a Viewlux reader (Perkin Elmer) with an integration time of 30 seconds per plate.

For single-agent studies, cells were treated with a 3-fold dilution series of eight concentrations of each drug, with six replicate treatments at each drug concentration per cell line. The starting concentrations were selected to span the IC_{50} in 96-hour proliferation assays based on our own or published data on each drug. Hierarchical clustering of single-agent response data demonstrates that drugs with similar mechanisms cluster together demonstrating the integrity of our results (Supplementary Fig. S1). For combination studies, cells were treated with a 4 by 4 matrix of drug concentrations also selected to span the IC_{50} for each drug (Supplementary Fig. S2) with four replicate treatments at each drug/drug combination concentration per cell line. In total, there were 60 assay plates per cell line screened and the typical throughput was five cell lines per day.

Reagents

Antibodies for Western blot analysis were all obtained from Cell Signaling Technology: pCdc2 cat. no. 9111, Cdc2 cat. no.9112, S6 ribosomal protein cat. no.2217, pS6 ribosomal protein cat. no. 2211, cleaved PARP cat. no. 9546.

In vitro cell viability

Cells were plated in 96-well plates at 3,500 cells/well. Cells were then treated with an eight by eight matrix of concentrations of the Wee1 inhibitor, AZD1775, and mTOR inhibitor, ridaforolimus. Ninety-six hours later, cell viability was measured using Cell Titer Glo (Promega).

In vivo efficacy

Six- to 8-week-old female athymic (CD1 nu/nu) mice from Charles River Laboratories were housed under pathogen-free conditions in microisolator cages with laboratory chow and water *ad libitum*. A total of 3×10^6 SK-OV-3 and A2780 cells in PBS: Matrigel (1:1) were injected subcutaneously into the right flank region. Tumors were allowed to reach 150 to 400 mm^3 for efficacy

Table 1. Thirty-eight compounds used in the combination screen

Compound	Target	Class
MK-2206	Protein kinase B (AKT)	Experimental
MK-4541	Anti-androgen	Experimental
MK-5108	Aurora kinase A	Experimental
Dinaciclib	Cyclin-dependent kinases (CDK)	Experimental
MK-8776	Checkpoint kinase 1 (Chk1)	Experimental
BEZ-235	Phosphatidylinositol-4,5-bisphosphate 3-kinase and mechanistic target of rapamycin (PI3K/mTOR)	Experimental
L-00778,123	Farnesyltransferase/GGPTase-I (FTI/GGTI)	Experimental
MRK-003	γ-secretase	Experimental
Geldanamycin	HSP90	Experimental
PD325901	MEK	Experimental
MK-8669	mTOR	Experimental
MK-4827	PARP	Experimental
ABT-888	PARP	Experimental
AZD1775	Wee1	Experimental
Metformin	5′ AMP activated kinase (AMPK) agonist	Approved
Methotrexate	Dihydrofolate reductase	Approved
Temozolomide	DNA	Approved
Mitomycin	DNA	Approved
Oxaliplatin	DNA	Approved
5-Fluorouracil	DNA/RNA	Approved
Lapatinib	EGFRs (EGFR/Her2)	Approved
Erlotinib	EGFR	Approved
Zolinza	Histone deacetylase (HDAC)	Approved
Paclitaxel	Microtubules	Approved
Vinblastine	Microtubules	Approved
Vinorelbine	Microtubules	Approved
Sorafenib	Multi-kinase	Approved
Dasatinib	Multi-kinase	Approved
Sunitinib	Multi-kinase	Approved
Dexamethasone	Glucocorticoid receptor	Approved
Bortezomib	Proteasome	Approved
Gemcitabine	Ribonucleotide reductase	Approved
SN-38	Topoisomerase I	Approved
Topotecan	Topoisomerase I	Approved
Doxorubicin	Topoisomerase II	Approved
Etoposide	Topoisomerase II	Approved

NOTE: Target corresponds to a drug target gene, protein, or organelle. Class represents approval status at time of submission.

Published OnlineFirst March 16, 2016; DOI: 10.1158/1535-7163.MCT-15-0843

studies (8–10 mice per group) or 350 to 600 mm^3 for mechanism of action studies (3 mice per group) before randomization. AZD-1775 was prepared in 0.5% methylcellulose. It was administered orally at 5 μL per gram of body weight (5 days on/2 days off). Ridaforolimus was prepared in 10% DMA (N,N-dimethyl acetamide), 10% Tween-80, 40% PEG-400, and 40% water. It was administered intraperitoneally at 5 μL per gram of body weight (5 days on/2 days off). SK-OV-3 mice were treated for 28 days (four cycles) for the tumor growth experiment while the mice received only one treatment for the mechanism of action study. A2780 mice were treated until individual tumor reached 1,000 mm^3 for the tumor growth experiment while the mice received only one treatment for the mechanism of action study. After treatment, mice were sacrificed with CO_2. The tumors were then removed and frozen in liquid nitrogen for future protein extraction for Western blot analysis. Twice a week, xenografts were measured with a caliper. Caliper measurements were used to calculate tumor volumes using the formula $V = \text{length} \times \text{width}^2 \times 0.5$.

Data analysis: calculation of normalized response and synergy

Assuming exponential growth, the number of cells at time t and 0 are defined by the expression $N(t)=N(t=0\ \text{h})\ ^{*}\ \exp(\text{mu}^{*}t)$, where mu is a growth constant that depends on individual cell line growth properties. Drug effect was measured by the ratio mu/muMax, where mu was the growth rate for cells treated with a drug and muMax for the cells treated with DMSO. For ease of use, mu/muMax was transformed into viability units $X/X_0=\exp(\ln(4)^{*}(\text{mu/muMax}))$. We have used two models to estimate synergy, highest single-agent (HSA) model, and the Bliss independence (10). The HSA model predicts the combined effect E_{AB} for two single compounds with effects E_A and E_B is $E_{AB}= \max(E_A,E_B)$. The Bliss model predicts the combined effect E_{AB} for two single compounds with effects E_A and E_B is $E_{AB}= E_A+ E_B - E_A \times E_B$, where each effect is expressed as a fractional inhibition between 0 and 1 at the same concentration as mixture. For both models, the synergy is calculated as the difference between the observed effect of the combination and the predicted effect E_{AB}.

Results

The OncoPolyPharmacology screen

In an effort to identify effective combinations for inhibiting growth of cancer cells in an unbiased manner, we screened 22 experimental drugs in all possible pairwise combinations as well as in combination with 16 approved drugs (Table 1) in a panel of 39 cancer cell lines (Supplementary Table S1) for a total of 583 combinations and 22,737 experiments (Supplementary Data). The compounds included experimental inhibitors of signaling molecules such as MEK and PI3K as well as approved drugs for the treatment of cancer such as paclitaxel and doxorubicin. The cancer cell lines chosen represent the most prevalent cancer types (lung, breast, ovarian, colon, melanoma, and prostate). Eight-point dose titrations of each drug were first performed on the 39 cell lines to identify the appropriate dose ranges to be used in the combination screening. For combination screening, compounds were tested in a 4 by 4 matrix of drug concentrations representative of the cell-active concentrations of each drug (Fig. 1A).

There are many methods available to evaluate drug combination responses. In our analysis, we used both the highest single agent (HSA) and Bliss independence models. In HSA, the effect of a drug combination is compared with the maximum effect of the individual component doses, whereas the Bliss model predicts the additive effect of two drugs acting independently. For both models, to capture effects across the entire 4 by 4 matrix, we used response surface methodology to quantitate volumetric predictions and observations (Fig. 1B). The single-agent drug effects were expressed as fractional inhibition between 0 (maximal inhibition) and 1 (no inhibition) relative to DMSO-treated controls, and these values were used at each drug concentration to calculate a predicted surface area based on HSA or Bliss model predictions (Fig. 1B, blue surface). Fractional inhibition by the

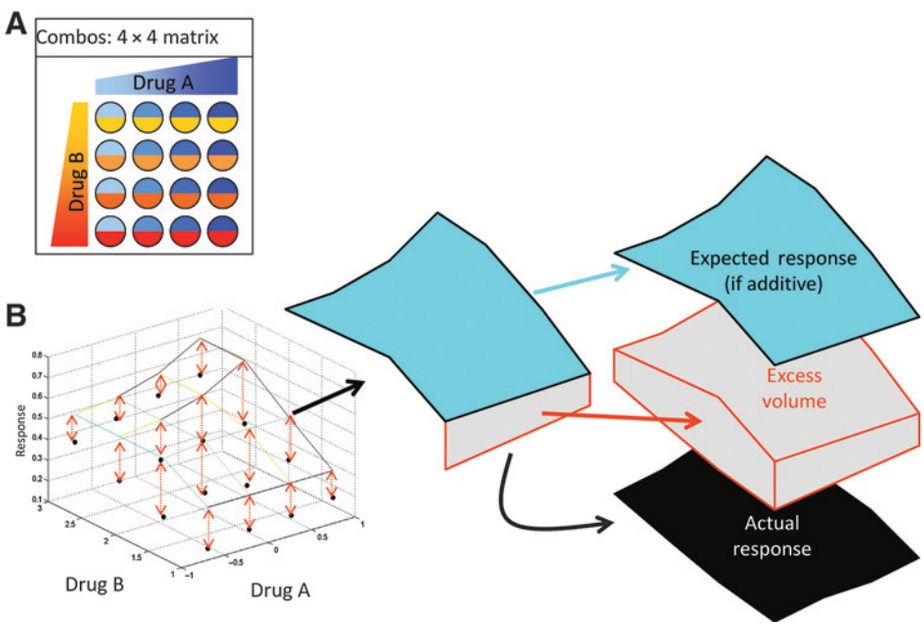

Figure 1.
The OncoPolyPharmacology Screen. A, drug pairs were screened in combination over fixed 4-point titrations (4 by 4 matrix, shown above) representative of the cell-active concentrations of each drug. Cell proliferation over 96 hours in the presence of drug, relative to vehicle, was determined with CellTiter Glo. B, using either the Bliss model or the highest single agent (HSA) model, additivity predictions could be made based on single-agent effects of the compounds (light blue surface). Actual effects observed are recorded (black surface) and the volumetric difference (gray space) is calculated as a measure of synergy, or combination activity exceeding the predicted outcome. Volume differences are assigned on the basis of the Bliss model (V_{Bliss}) or the HSA model (V_{HSA}).

Published OnlineFirst March 16, 2016; DOI: 10.1158/1535-7163.MCT-15-0843

drug combinations was similarly used to calculate observed surface areas (Fig. 1B, black surface). From these values, volumetric effects for each combination were calculated by subtracting the actual response from the predicted response and expressed as either V_{HSA} or V_{Bliss} (Fig. 1B, gray volume).

Both V_{HSA} and V_{Bliss} models had a narrow distribution with V_{HSA} centered at 0.04 and V_{Bliss} centered at 0.007. These distributions clearly suggest that synergy and antagonism are rare events. Because of the variability in drug–response data, antagonism was defined arbitrarily as $V_{HSA} < -0.12$ and synergy as $V_{Bliss} > 0.12$. Additive combinations were defined as $V_{HSA} > 0.12$ and $V_{Bliss} < 0.12$.

Landscape of combination synergy and response

In our dataset, the majority of the drug combinations showed no synergy (Fig. 2A and B) in one or more cell lines. Synergistic ($V_{Bliss} > 0.12$) or antagonistic ($V_{HSA} < -0.12$) combinations were observed much less frequently at 0.05% and 0.01%, respectively. To visualize combinations with synergy across multiple cell lines, a heatmap illustrating the number of cell lines with synergy for each pairwise combination is shown (Fig. 2C). A similar heatmap was also generated for antagonism (Fig. 2D). As mentioned above, antagonism and synergy are rare events. However, many combinations can be found that have synergy or antagonism in at least one cell line. Of the 538 combinations tested, 287 (~50%) were synergistic in at least one cell line and 178 (~30%) were antagonistic in at least one cell line. We identified few broadly synergistic combinations including the Wee1 inhibitor combined with the Chk1 inhibitor (11) and PARP inhibitor combined with temozolimide (12, 13). Context-dependent synergistic drug combinations were also identified, including the mTOR inhibitor/AKT inhibitor combination and mTOR inhibitor/ERK inhibitor combination.

The aforementioned synergistic combinations have biologic rationale supporting them and therefore might have been predicted. However, the unbiased nature of the screen allowed us to identify novel combinations that one would not have necessarily predicted on the basis of our current understanding of the mechanisms of action of each agent. Examples of such novel synergistic combinations include the HSP inhibitor with the farnesyl transferase inhibitor, the MEK inhibitor with vinblastine, and the Wee1 inhibitor with the mTOR inhibitor (Fig. 2D). Because of the novelty at the time of the screen as well as the advanced stage of each compound in clinical development, we chose to further validate and characterize the Wee1 inhibitor (14)/mTOR inhibitor (15) combination.

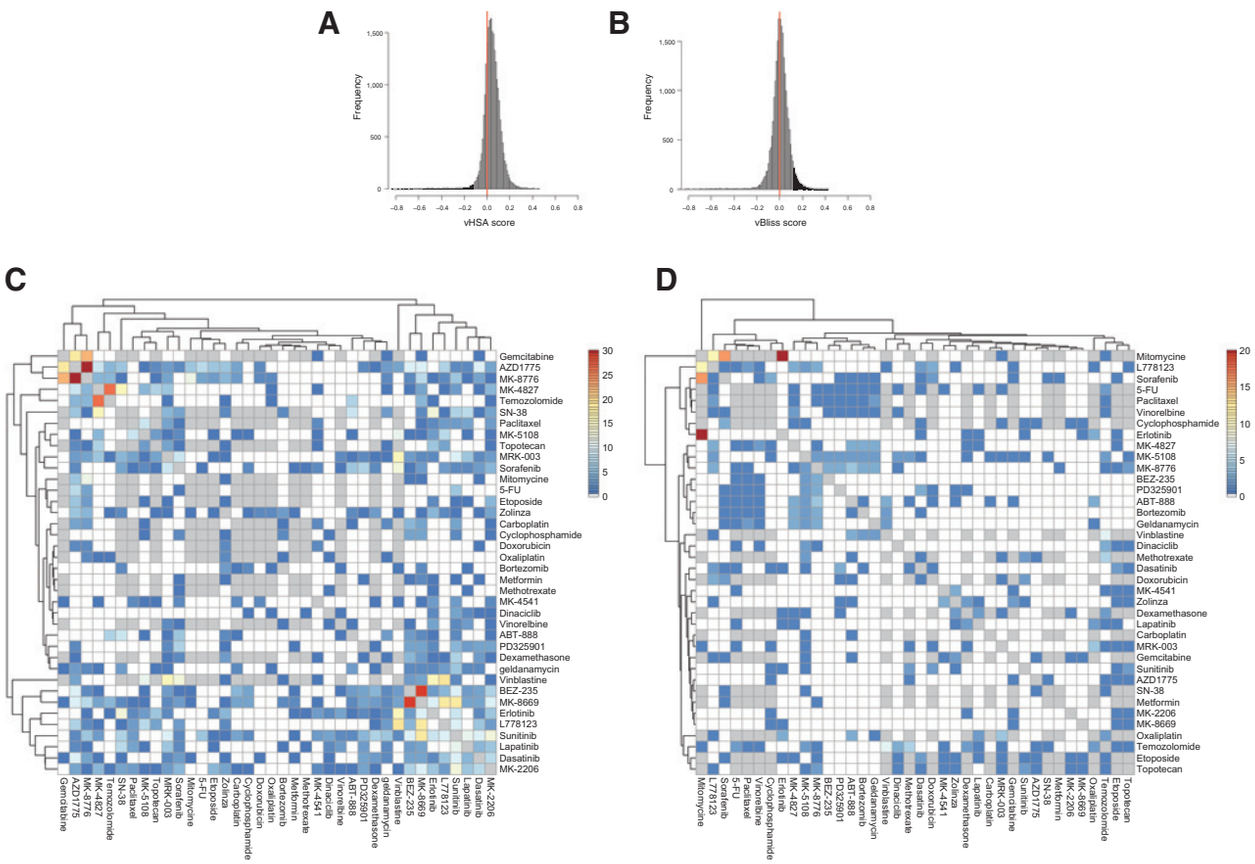

Figure 2.
Global view of synergy and antagonism. A, V_{HSA} score distribution across 22,737 experiments. B, V_{Bliss} score distribution across 22,737 combination experiments. C, heatmap indicating the number of cell lines where synergy was observed for each combination (scale to the right). The cutoff for synergy was $V_{Bliss} > 0.12$. D, heatmap indicating the number of cell lines where antagonism was observed for each combination. The cutoff for antagonism was $V_{HSA} < -0.12$. Gray indicates untested combinations.

Published OnlineFirst March 16, 2016; DOI: 10.1158/1535-7163.MCT-15-0843

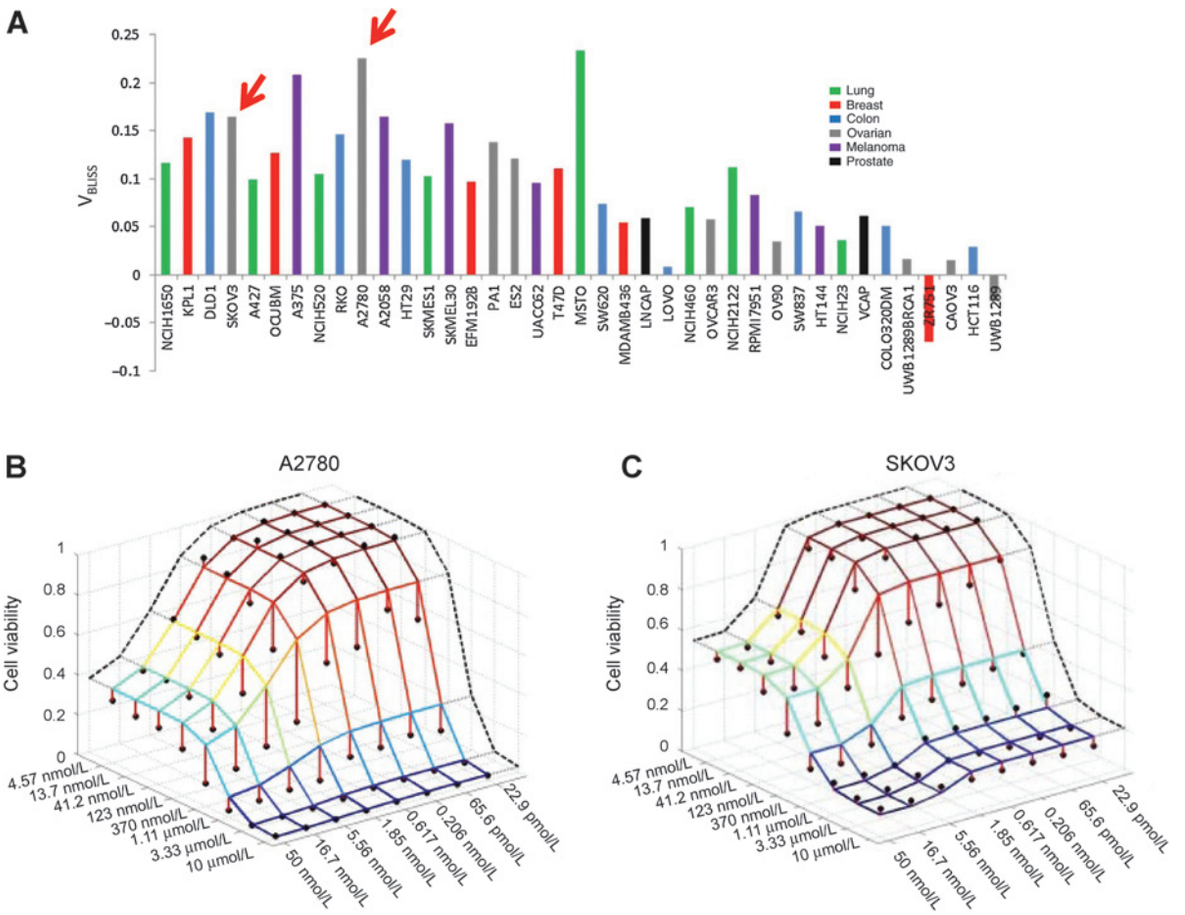

Figure 3.
Wee1i + mTORi is a synergistic combination *in vitro*. A, synergy scores (V_{Bliss}) were plotted for the combination of a Wee1 inihbitor (AZ1775) and mTOR inhibitor (ridaforolimus) among each of the 39 cell lines screened. Cell lines were colored according to tissue of origin. B and C, two ovarian cancer cell lines where synergy was observed, A2780 and SKOV-3, were selected for follow-up validation. Surface plots for cell viability relative to vehicle treatment in an 8-point titration combination for the Wee1 and mTOR inhibitors. The predicted effect (Bliss synergy model) of the combination on cell viability is represented by the top surface, and observed effect on cell viability is demonstrated by the black points on the graph.

Characterization of the novel Wee1 inhibitor/mTOR inhibitor combination

The combination of the Wee1 inhibitor and mTOR inhibitor was identified in the primary screen as synergistic in multiple cell lines and indications (Fig. 3A). To validate these primary screen results, we treated two cell lines in which the combination was synergistic, A2780 and SKOV3, with an 8 by 8 dose titration matrix of these compounds. Viability was then assessed 96 hours posttreatment. As shown in Fig. 3B, the expected versus observed surface plot of the 8 by 8 matrix viability data demonstrates synergy at multiple doses.

To further explore the Wee1 inhibitor and mTOR inhibitor combination, the tolerability of combining these two agents *in vivo* was determined. When mice were codosed with the MTDs of the monotherapies, the combination produced some body weight loss but was tolerated (Fig. 4A). To investigate the *in vivo* activity of this combination, efficacy was tested for the monotherapies and combination in two xenograft models of ovarian cancer. These models were selected on the basis of their robust *in vitro* synergy and response. For the A2780 xenograft model, mice were dosed for 3 weeks. The Wee1 inhibitor and mTOR inhibitor combination significantly inhibited tumor growth compared with either monotherapy ($P = 0.0066$ and 0.0063 compared with mTOR inhibitor alone and Wee1 inhibitor alone, respectively; Fig. 4B). The combination resulted in 71% tumor growth inhibition at the end of the dosing period compared with 14% and 12% for monotherapy arms of the study. After the 3-week dosing period, mice were monitored until their tumors reached 1,500 mm^3. The time for the tumors in combination-treated mice to reach 1,500 mm^3 was significantly longer (61 days) than the tumors in mice treated with either Wee1 inhibitor or mTOR inhibitor monotherapies (36, 50 days, respectively; $P = 0.005$ and <0.0001 compared with mTOR inhibitor alone and Wee1 alone, respectively; Fig. 4C). To further test the efficacy of the combination in an additional ovarian cancer model, we treated mice bearing SKOV3 ovarian xenograft tumors. We again found that the combination was significantly better in inhibiting tumor growth than either monotherapy in this model. The combination inhibited tumor growth by 95% at the end of the 4-week dosing period compared with 71% and 62% for the Wee1 inhibitor and mTOR inhibitor, respectively ($P = 0.0282$ and 0.0508

Published OnlineFirst March 16, 2016; DOI: 10.1158/1535-7163.MCT-15-0843

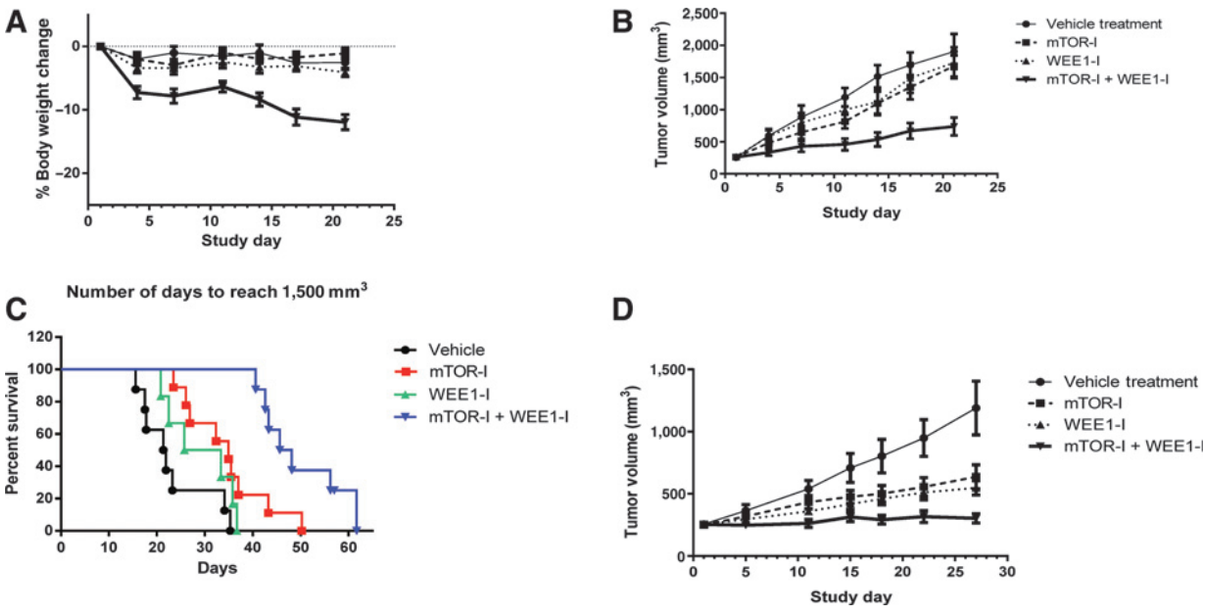

Figure 4.
The Wee1i + mTORi combination is well tolerated and provides a combination benefit in efficacy and survival over monotherapies alone. A, A2780 xenograft tumor-bearing mice ($n = 10$ per cohort) were treated with a Wee1 inhibitor (AZD-1775) at 60 mg/kg twice daily (5 days on, 2 days off), an mTOR inhibitor (ridaforolimus) at 1 mg/kg once daily (5 days on, 2 days off), or the combination of the Wee1 and mTOR inhibitors at the same doses and schedules for 3 weeks and relative body weight loss was monitored over the course of treatment. B, efficacy data for the experiment described in A. C, survival of A2780 tumor-bearing mice following the 3-week dosing period described in B. D, efficacy data for the Wee1i/mTORi combination in the SKOV3 xenograft model.

compared with mTOR inhibitor alone and Wee1 inhibitor alone respectively; Fig. 4D).

To explore potential mechanisms of action of the Wee1 inhibitor and mTOR inhibitor combination, we performed an acute pharmacodynamic study in mice bearing A2780 xenograft tumors. Mice were given 1 dose of either the Wee1 inhibitor (60 mg/kg), the mTOR inhibitor (1 mg/kg), or the combination. Mice were sacrificed 4 or 24 hours after treatment. As expected, we found that the levels of pS6 ribosomal protein were reduced in tumors from mice treated with the mTOR inhibitor (Fig. 5). Likewise, we observed decreased levels of pCdc2 in tumors from mice treated with the Wee1 inhibitor for 4 hours. Surprisingly, we found that in mice treated with the combination, the phosphorylated S6 ribosomal protein levels were lower than in mice treated with the mTOR inhibitor alone. In addition, phosphorylated Cdc2 levels were lower in mice treated with the combination than in mice treated with the Wee1 inhibitor at the 4-hour timepoint. These results suggest a previously unknown interaction between the mTOR and DNA damage pathways. We also observed increased levels of cleaved PARP indicating increased levels of apoptosis in tumors from mice 24 hours after treatment with the combination compared with tumors from mice treated with vehicle or either monotherapy.

Discussion

We have shown here through an unbiased large-scale combinatorial screening campaign that synergistic and efficacious

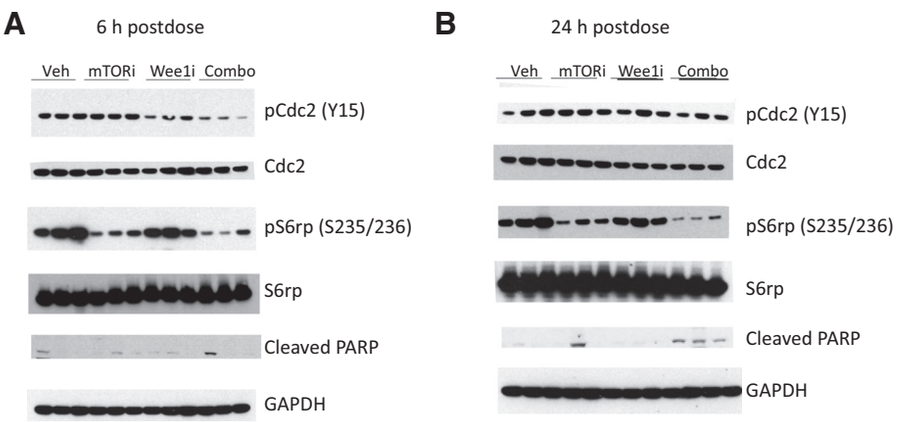

Figure 5.
Mice bearing A2780 xenograft tumors were treated with a single dose of a Wee1 inhibitor (AZD-1775) at 60 mg/kg, an mTOR inhibitor (ridaforolimus) at 1 mg/kg, or the combination of the Wee1 and mTOR inhibitors at the same doses. Three mice in each group were sacrificed at either 6 (A) or 24 hours (B) following the dosing and tumors were harvested for Western blot analysis with the indicated antibodies.

Published OnlineFirst March 16, 2016; DOI: 10.1158/1535-7163.MCT-15-0843

combination pairs can be identified. Our primary objective was to identify novel combinations that would not have been appreciated simply by using pathway knowledge to guide combination testing. We have discovered several novel combinations using this methodology and have presented here in detail the characterization of the Wee1i + mTORi combination.

Several important findings can be concluded from the data presented here. First, combination synergy and antagonism are a relatively infrequent phenomenon. Second, compounds that have multiple targets (i.e., sunitinib, sorafenib) frequently combine synergistically with multiple compounds with unrelated mechanisms of action. While this observation is intuitive, it has not been demonstrated systematically in a large combination screen, as reported here. Third, in addition to intra-pathway synergistic combinations (PI3K + PI3K pathway inhibitors, MAPKi + MAPKi pathway inhibitors, and DNA damage/cell-cycle checkpoint pathway combinations), which is consistent with a wealth of publications demonstrating intrapathway synergy (16), we also discovered novel interpathway combinations. Although broadly synergistic combinations may seem the most attractive, we suspect that many of these combinations may not be well tolerated in mice and human patients. Notably, the mTOR inhibitor/Wee1 inhibitor combination was well tolerated at the respective MTDs while the Chk1 inhibitor/Wee1 inhibitor was not (11, 17). Context-dependent combinations, especially those that combine drugs targeting two different pathways, are less likely to have overlapping toxicities.

The Wee1i + mTORi combination was identified in the primary screen and would not have been obvious from known mechanisms of action of both compounds. Wee1 is a central regulator of CDK1/2 and prevents premature CDK activation in unperturbed DNA replication as well as in the presence of DNA-damaging agents (18–20). In contrast, mTOR is a central mediator of the PI3K pathway and has roles in controlling cell growth and proliferation (21–23). That said, it is well established that cells precisely couple cell growth with cell division. Therefore, at a high level, the general mechanism accounting for the observed synergy/efficacy may be related to uncoupling the regulation of cell growth and cell division.

The precise mechanism of action for the Wee1i + mTORi combination remains to be determined. However, data presented here indicate that there may be effects on the PI3K pathway after treatment with the Wee1 inhibitor. In the context of the combination, we found more robust inhibition of phospho-S6. Conversely, we also found that the combination more robustly inhibited phospho-Cdc2. Therefore, previously unknown interactions between the mTOR and Wee1 pathways may account for the synergy and increased efficacy.

While we were preparing this manuscript, another group identified the Wee1i + mTORi combination in a screen to identify compounds that enhance the activity of the mTOR inhibitor, Torin, in RAS-mutant leukemia (24). In our work, we show that although the combination is efficacious in a context-dependent manner, combination benefit is not exclusively observed in RAS-mutant cancer cell lines or in cell lines with high RAS signature (Supplementary Table S1), which we believe is a better predictor of RAS pathway activation (25). Because the cell line panel used here consisted of only 39 cell lines in six different indications, it was not powered to determine responder populations/predictive biomarkers. We are in the process of using a large cell line panel to determine biomarkers predictive of combination response for the Wee1i +mTORi combination as well as other combinations of interest.

Disclosure of Potential Conflicts of Interest

No potential conflicts of interest were disclosed.

Authors' Contributions

Conception and design: J. O'Neil, I. Feldman, B. Roberts, J. Li, A. Kral, W. Arthur, C. Winter, A. Bloecher, S.D. Shumway

Development of methodology: Y. Benita, I. Feldman, M. Chenard, B. Roberts, Y. Liu, S. Lejnine, W. Arthur

Acquisition of data (provided animals, acquired and managed patients, provided facilities, etc.): J. O'Neil, M. Chenard, B. Roberts, Y. Liu, J. Li, W. Arthur, B.B. Haines

Analysis and interpretation of data (e.g., statistical analysis, biostatistics, computational analysis): J. O'Neil, Y. Benita, I. Feldman, M. Chenard, B. Roberts, Y. Liu, J. Li, S. Lejnine, A. Loboda, W. Arthur, R. Cristescu, B.B. Haines, C. Winter, T. Zhang, A. Bloecher, S.D. Shumway

Writing, review, and/or revision of the manuscript: J. O'Neil, Y. Benita, I. Feldman, M. Chenard, B. Roberts, Y. Liu, J. Li, S. Lejnine, R. Cristescu, B.B. Haines, C. Winter, A. Bloecher, S.D. Shumway

Administrative, technical, or material support (i.e., reporting or organizing data, constructing databases): J. O'Neil, Y. Benita

Study supervision: A. Kral, S.D. Shumway

The costs of publication of this article were defrayed in part by the payment of page charges. This article must therefore be hereby marked *advertisement* in accordance with 18 U.S.C. Section 1734 solely to indicate this fact.

Received October 29, 2015; revised February 15, 2016; accepted March 7, 2016; published OnlineFirst March 16, 2016.

References

1. Workman P, Al Lazikani B, Clarke PA. Genome-based cancer therapeutics: targets, kinase drug resistance and future strategies for precision oncology. Curr Opin Pharmacol 2013;13:486–96.
2. Lito P, Pratilas CA, Joseph EW, Tadi M, Halilovic E, Zubrowski M, et al. Relief of profound feedback inhibition of mitogenic signaling by RAF inhibitors attenuates their activity in BRAFV600E melanomas. Cancer Cell 2012;22:668–82.
3. Frei EIII. Combination chemotherapy of acute leukemia and Hodgkin's disease. JAMA 1972;222:1168.
4. Peters S, Bouchaab H, Zimmerman S, Bucher M, Gaide O, Letovanec I, et al. Dramatic response of vemurafenib-induced cutaneous lesions upon switch to dual BRAF/MEK inhibition in a metastatic melanoma patient. Melanoma Res 2014;24:496–500.
5. Barretina J, Caponigro G, Stransky N, Venkatesan K, Margolin AA, Kim S, et al. The Cancer Cell Line Encyclopedia enables predictive modelling of anticancer drug sensitivity. Nature 2012;483:603–7.
6. Garnett MJ, Edelman EJ, Heidorn SJ, Greenman CD, Dastur A, Lau KW, et al. Systematic identification of genomic markers of drug sensitivity in cancer cells. Nature 2012;483:570–5.
7. Held MA, Langdon CG, Platt JT, Graham-Steed T, Liu Z, Chakraborty A, et al. Genotype-selective combination therapies for melanoma identified by high-throughput drug screening. Cancer Discov 2013;3:52–67.
8. Roller DG, Axelrod M, Capaldo BJ, Jensen K, Mackey A, Weber MJ, et al. Synthetic lethal screening with small-molecule inhibitors provides a pathway to rational combination therapies for melanoma. Mol Cancer Ther 2012;11:2505–15.
9. Kang Y, Hodges A, Ong E, Roberts W, Piermarocchi C, Paternostro G. Identification of drug combinations containing imatinib for treatment of BCR-ABL+ leukemias. PLoS ONE 2014;9:e102221.
10. Borisy AA, Elliott PJ, Hurst NW, Lee MS, Lehar J, Price ER, et al. Systematic discovery of multicomponent therapeutics. Proc Natl Acad Sci U S A 2003;100:7977–82.

Published OnlineFirst March 16, 2016; DOI: 10.1158/1535-7163.MCT-15-0843

11. Guertin AD, Martin MM, Roberts B, Hurd M, Qu X, Miselis NR, et al. Unique functions of CHK1 and WEE1 underlie synergistic anti-tumor activity upon pharmacologic inhibition. Cancer Cell Int 2012;12:45.
12. Plummer R, Jones C, Middleton M, Wilson R, Evans J, Olsen A, et al. Phase I study of the poly(ADP-ribose) polymerase inhibitor, AG014699, in combination with temozolomide in patients with advanced solid tumors. Clin Cancer Res 2008;14:7917–23.
13. Plummer R, Stephens P, Aissat-Daudigny L, Cambois A, Moachon G, Brown PD, et al. Phase 1 dose-escalation study of the PARP inhibitor CEP-9722 as monotherapy or in combination with temozolomide in patients with solid tumors. Cancer Chemother Pharmacol 2014;74:257–65.
14. Hirai H, Iwasawa Y, Okada M, Arai T, Nishibata T, Kobayashi M, et al. Small-molecule inhibition of Wee1 kinase by MK-1775 selectively sensitizes p53-deficient tumor cells to DNA-damaging agents. Mol Cancer Ther 2009;8:2992–3000.
15. Metcalf CA, Bohacek R, Rozamus LW, Burns KD, Roses JB, Rivera VM, et al. Structure-based design of AP23573, a phosphorus-containing analog of rapamycin for anti-tumor therapy. Proc Amer Assoc Cancer Res 2004;45:2476.
16. Al Lazikani B, Banerji U, Workman P. Combinatorial drug therapy for cancer in the post-genomic era. Nat Biotechnol 2012;30:679–92.
17. Guertin AD, Li J, Liu Y, Hurd MS, Schuller AG, Long B, et al. Preclinical evaluation of the WEE1 inhibitor MK-1775 as single-agent anticancer therapy. Mol Cancer Ther 2013;12:1442–52.
18. Raleigh JM, O'Connell MJ. The G(2) DNA damage checkpoint targets both Wee1 and Cdc25. J Cell Sci 2000;113:1727–36.
19. Beck H, Nahse V, Larsen MS, Groth P, Clancy T, Lees M, et al. Regulators of cyclin-dependent kinases are crucial for maintaining genome integrity in S phase. J Cell Biol 2010;188:629–38.
20. Dominguez-Kelly R, Martin Y, Koundrioukoff S, Tanenbaum ME, Smits VA, Medema RH, et al. Wee1 controls genomic stability during replication by regulating the Mus81-Eme1 endonuclease. J Cell Biol 2011;194:567–79.
21. Hay N, Sonenberg N. Upstream and downstream of mTOR. Genes Dev 2004;18:1926–45.
22. Shaw RJ, Cantley LC. Ras, PI(3)K and mTOR signalling controls tumour cell growth. Nature 2006;441:424–30.
23. Schmelzle T, Hall MN. TOR, a central controller of cell growth. Cell 2000;103:253–62.
24. Weisberg E, Nonami A, Chen Z, Liu F, Zhang J, Sattler M, et al. Identification of Wee1 as a novel therapeutic target for mutant RAS-driven acute leukemia and other malignancies. Leukemia 2015;29:27–37.
25. Loboda A, Nebozhyn M, Klinghoffer R, Frazier J, Chastain M, Arthur W, et al. A gene expression signature of RAS pathway dependence predicts response to PI3K and RAS pathway inhibitors and expands the population of RAS pathway activated tumors. BMC Med Genomics 2010;3:26.

Published OnlineFirst March 16, 2016; DOI: 10.1158/1535-7163.MCT-15-0843

Molecular Cancer Therapeutics

An Unbiased Oncology Compound Screen to Identify Novel Combination Strategies

Jennifer O'Neil, Yair Benita, Igor Feldman, et al.

Mol Cancer Ther 2016;15:1155-1162. Published OnlineFirst March 16, 2016.